

Electric Field Servoing for Robotic Manipulation

Ryan Wistort, Joshua R. Smith

Abstract—This paper presents two experiments with Electric Field Servoing for robotic manipulation. In the first, a robot hand pre-shapes to the geometry and pose of objects to be grasped, by servoing each finger according to the values on EF sensors built in to each finger. In the second, a 7 degree of freedom arm aligns itself in 2 dimensions with a target object using electric field measurements as the error signal. This system also allows the end effector to dynamically track the target object as it is moved.

I. INTRODUCTION

Visual Servoing[1] is the use of feedback from a machine vision system to correct the position of a robot in order to increase task accuracy. This paper explores the use of Electric Field Pretouch[2] as the feedback signal for closed loop control in robotic manipulation tasks. While it is possible to solve a compute-intensive inverse problem to infer explicit geometrical information from an array of electric field measurements[3], this paper shows that useful results can be achieved using closed loop control schemes based on electric field sensor values that are subject to only minimal computational processing.

In the first experiment, a robotic hand uses Electric Field servoing to pre-shape to an object. Uncertainties in object pose are readily accommodated with this technique, and as long as the hand is in pre-shaping mode, the hand will dynamically compensate for changes in object pose or geometry (for example, if the object is suddenly replaced by a different one). By adjusting the set point to which the fingers are servoing, the hand can be made to grasp the object. In the second experiment, EF sensors on the end effector of a robotic arm are used to correct its position after execution of a trajectory that brings the end effector near the object. Our intended usage model is that a vision system (with an overhead camera) will provide an initial estimate of object position. Then a global planner will generate a trajectory that brings the end effector near the object. Once this trajectory has executed (possibly with actuation or vision errors), the arm will in some cases occlude the overhead camera's view of the object. The EF-servoing

Manuscript received February 22, 2007. This work was supported by Intel Research.

Ryan Wistort is an intern at Intel Research Seattle (email: Ryan@RyBOTS.com).

Joshua R. Smith is a Principal Engineer at Intel. Address: Intel Research Seattle, WA 98105 USA (corresponding author Phone: 206-633-9900; fax: 206-633-6504; e-mail: joshua.r.smith@intel.com).

process will then correct the position of the end effector, regardless of whether the arm has occluded the camera's view of the target object.

In future work, we intend to combine these two experimental systems, by mounting the EF-sensing hand on the arm. Then the EF sensors in the hand will perform both arm alignment correction, and grasp pre-shaping.

II. ELECTRIC FIELD SENSING

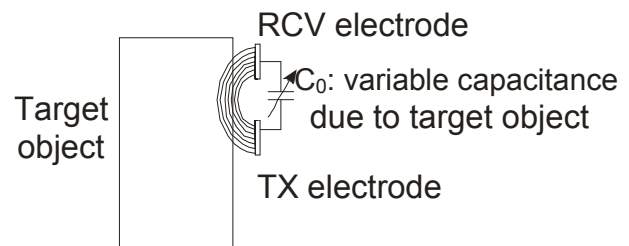


Fig. 1: Schematic representation of a single electric field sensing channel. If the target object is within the sensor electrode pair's field of view, then as the sensor-to-object spacing changes (or more generally, as the geometry changes), the signal at the receive electrode changes.

In Electric Field Sensing, illustrated in Figure 1, a low frequency (100KHz) AC voltage is applied to a transmit electrode (labeled TX), which via capacitance C_0 induces a displacement current in the receive electrode (labeled RCV).[2] The position of the target object relative to TX and RCV modifies the capacitance C_0 between TX and RCV, and thus the amplitude of the signal received at RCV. If the target object is well-coupled to ground, the displacement current received at RCV decreases as the electrodes approach the object.

Electric Field Sensing is well-suited to measuring conductive objects, as well as objects whose dielectric constant is substantially different than the surroundings. In practice, metals, the human body, fruits and vegetables, and water-based liquids all work well because of their high conductivity and/or dielectric contrast. Thin plastic cases, fabric, thin sheets of paper and thin glass cannot be sensed well (thin means relative to the electrode spacing). On the positive side, this means that Electric Field Sensing can operate through thin layers of plastic, fabric, paper, or glass if desired. In this paper, we make use of this last property by sensing through plastic fingertips.

If Electric Field Pretouch proves useful for manipulation, we plan to explore other pretouch mechanisms that will work with objects that EF sensing cannot readily detect.

III. RELATED WORK

Electric Field Pretouch was introduced in [2], which presented several preliminary experiments with the use of Electric Field sensing for robotic manipulation, and focused on showing that arrays of field measurements contain sufficient information to distinguish object size and object distance. Reference [2] includes a 1D arm alignment experiment using a simple 3DOF planar manipulator. The present paper generalizes the 1D differential electrode geometry of [2] to 2D, and demonstrates arm alignment in two dimensions using a 7DOF arm, a much more compelling usage. Although [2] included a very simple two-fingered “hand” prototype, this device was not capable of grasping, and the concept of EF Servoing for grasp pre-shaping was not discussed. Also, in [2] one finger contained the TX electrode and the other contained the RCV electrode; in the present paper, each finger contains a TX-RCV pair, which provide much more useful geometrical information. The hand pre-shaping presented in the present paper could not have been accomplished with the electrodes of [2].

Electric Field and capacitive sensing has been explored in robotics in the contexts of whole arm obstacle avoidance, safety, and seam-following. Novak and Feddema [4] described an 8 channel Electric Field sensor system for obstacle avoidance in a whole-arm manipulator. Karlsson [5] described a capacitive safety system that shuts down a robot if a human enters its workspace. Schmitt et al. [6] described a capacitance-based seam tracking system for dispensing brazing paste with high precision and high speed for rocket thrust chamber manufacturing. Mauer [7] described an end effector with an array of single-electrode capacitive sensors. The sensor information from the array was used only to form an “image,” and was not used for control purposes. More recently, Solberg, Lynch, and MacIver demonstrated robotic electrolocation for an underwater robot.[8]

IV. EF SERVOING FOR HAND PRESHAPING

For this experiment, the metal fingertips of a Barrett Hand were replaced by 3D-printed plastic fingertips. It was desirable to switch to plastic because it does not interact strongly with electric fields, so the electrodes could be mounted on the back side of the plastic finger surface. A Transmit-Receive pair of electrodes was mounted in each finger. As shown in the figure, the transmit (TX) electrode was mounted on the inner “pad” surface of the finger, and the receive (RCV) electrode was mounted inside the top of the fingertip. This geometry was chosen because it produces high field strength (and thus sensitivity) at the fingertip. In an earlier attempt at an EF Sensing fingertip, the TX electrode was placed in the same position as in the figure, but the RCV electrode was parallel to the TX electrode, just above it on the interior of the finger “pad” surface. This geometry yielded much less sensitivity near the finger tip. There is one other crucial electrode design choice: in the

absence of noise, the TX and RCV electrodes would produce the same signal if interchanged, because of reciprocity. However, the RCV electrode is highly sensitive to electrical noise, and the TX electrode is insensitive to noise. The pulse width modulated motor control signals inside the hand produce substantial electrical noise. Thus it turns out that interchanging the electrodes would result in much higher noise levels, because the sensitive RCV would be closer to the noise sources in the hand.

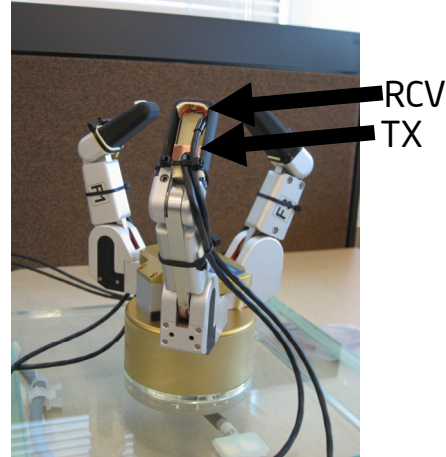


Fig. 2: EF Sensing robotic hand. The original metal fingertips were replaced with plastic, and a Transmit-Receive electrode pair was mounted in each fingertip.

The sensing for the pre-shaping experiment was implemented with two LazyFish Electric Field Sensing boards, described in [2]. The LazyFish board provides 4 TX channels and only 2 RCV channels. Since each finger has a receiver, two boards were necessary to make the desired measurements.

The sensor values were filtered using the following Infinite Impulse Response filter:

$$S_t = \alpha S_{t-1} + (1 - \alpha) R_t$$

where R_t is the newest “raw” sensor value, and S_{t-1} is the previous filtered value. Because of the substantial motor noise, we set $\alpha=0.8$, which provides aggressive low pass filtering.

Fig. 3 illustrates the response of the sensors for several objects. To collect the data, an object was placed on the palm of the hand. Then each finger was commanded by the experimenter to move very close to the object (about 1mm away). The experimenter verified the position of each finger visually and adjusted the finger angles until each finger tip was the desired distance from the object. Then the EF Sensor values on the 3 fingers were measured and logged, and the finger joints were commanded to open by 300 encoder counts. The sensor values were logged again, and the procedure was repeated until all three fingers were within 300 encoder counts of fully open. Thus the data in Fig. 3 was recorded from right to left. The end point for each finger (first encoder value less than 300) depends on

the start point for the finger, which is why the traces for each finger and each trial are slightly different near 0.

This data collection procedure (moving the fingers from near to far) was implemented so that the data could easily be used for calibration purposes. (Although we show data for several objects, the EF Servoing results, for multiple objects, were all achieved with the same calibration setting. The calibration was not changed for different objects.)

The left column of the figure shows the data for (1) an aluminum can oriented vertically, (2) the can resting on its side, (3) a plastic bottle containing water oriented vertically, (4) the same bottle resting on its side, (5) a metal can of “dust off” (liquid air), and (6) an ellipsoidal plastic bottle containing liquid soap (oriented vertically).

Examining the plot from left to right, It is apparent that the sensor channels in each finger have different baseline values. This is largely because of slight differences in electrode geometry: electrode pairs that are closer together will have higher baseline coupling.

The right column of Fig. 3 shows the derivative of sensor value with finger position (encoder value). Notice that this effectively eliminates the baseline dependencies

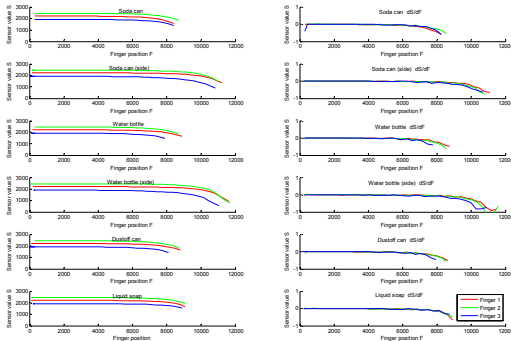


Fig. 3: Left column: the raw sensor response for several different objects. Right column: derivative of sensor response with finger position.

To implement pre-shaping, EF set point values are chosen for each finger. Fig. 3 shows that because of the varying baseline values, a different set point is required for each finger. (By servoing to derivative values, shown in the right column, finger-independent set points could probably be formulated.) Note that these set point values do not correspond directly to a distance from the object. As shown in [2], a small object close to a sensor pair can produce the same value as a large object further away. This means that the pre-shaping distance can vary somewhat with object size. If the EF set points are chosen so that the fingers do not touch the object for the smallest object of interest, then the fingers should not collide with any objects of interest (because larger objects will have larger pre-shaping distances, i.e. the finger position set points will be further from the object).

Fig.4 illustrates EF pre-shaping. The EF set points were chosen using calibration data of Fig. 3 so that the fingers would servo to about 1cm from the object. When the pre-shaping servo loop is activated, the fingers begin closing.

We used the Barrett Hand’s velocity control mode, in which a velocity is commanded, and position feedback is returned. We implemented a simple controller, with velocity proportional to the error signal. The hand’s position feedback was displayed but not used for control purposes. Only the error signals derived from the EF sensor values were used by the control loop. Note however that the position feedback provides very useful and nicely linear geometrical information that may be of interest in its own right.

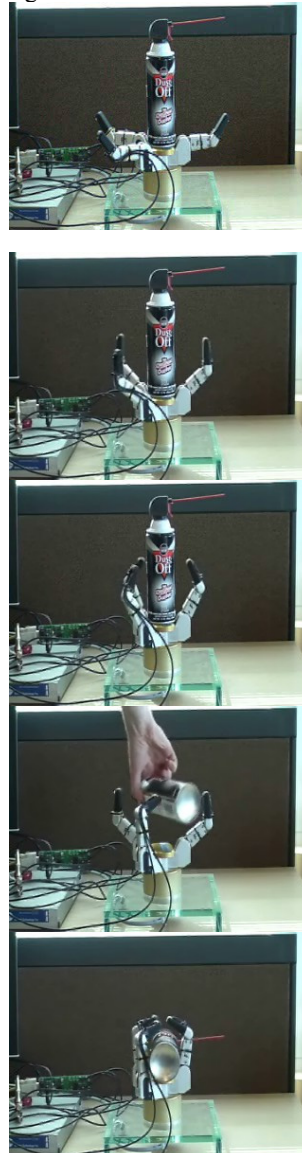


Fig. 4: EF pre-shaping. The fingers move toward the object (images 1 and 2) until they reach their set point (image 3). As the object’s pose is changed (image 4), the fingers adjust, opening or closing as necessary. When the object is in a new stable configuration, the fingers stabilize in the new configuration (image 5).

The video shows the EF pre-shaping hand in operation. In the video, several different objects are placed in the hand, which pre-shapes to each one. One of the fingers can be

observed “tapping” the object. This is hunting behavior due to a slightly mis-tuned control loop.

V. EF SERVOING FOR ARM ALIGNMENT

In the next experiment, EF sensors were used to servo the 2D position of a robot arm end effector to align with target objects. We used the Barrett WAM arm with 7 degrees of freedom. For this experiment, we constructed an electrode array consisting of a single circular receive electrode (RCV1) in the center, and 4 transmit electrodes placed around the receive at 0 degrees (TX1), 90 degrees (TX2), 180 degrees (TX3), and 270 degrees (TX4). The receive electrode is shielded from motor noise by a ground disk. The electrode array is illustrated in Fig. 5.

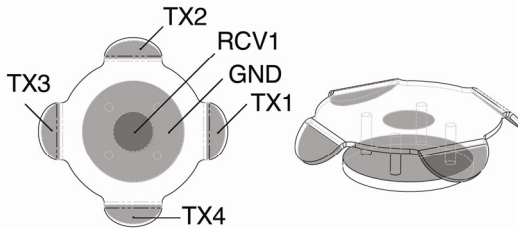


Fig. 5: Design of electrode array for arm alignment experiment. The large disk at the base is grounded, to shield the receive electrode (upper disk) from motor noise. The transmit electrodes are arrayed around the outside. The outward tilt of the transmit electrodes is designed to increase the sensing range.

The sensing instrumentation was a single LazyFish EF Sensor board, which time-multiplexes the TX electrodes. Thus the sensor board collects a first measurement from the TX1 RCV1 pair, followed by a second measurement from the TX2 RCV1 pair, and so on. When a symmetrical object is aligned symmetrically with the electrode pairs, they yield the same signal. Thus the imbalance between the TX1 RCV1 sensor pair and the TX3 RCV1 sensor pair can serve as the x error signal, and the imbalance between TX2 RCV1 and TX4 RCV1 pairs serves as the y error signal.

The x error signal is used to generate a an x position correction, and the y error signal generates a y position correction in the task space. The error signal is linearly scaled by a constant factor (chosen as a calibration step) to convert EF sensor values to end effector position changes. An inverse kinematics calculation is performed to derive new target joint angles from the new end effector target position.

A complete set of new EF Sensor values are collected at about 30Hz, and new arm target configurations are computed at this rate. The arm motion control is implemented by our own custom Virtual Series Elastic Actuator (VSEA) controller, which runs at approximately 500Hz on the Barrett WAM arm’s dedicated control PC. In the terminology of [1], this makes our system a “dynamic look and move” architecture, rather than a “direct EF servo” architecture. The VSEA controller effectively stabilizes the arm dynamics, since the EF

sensor update rate is slower than the arm motion control update rate.

Fig. 6 illustrates the EF servoing of the arm end effector. The arm executes a pre-planned trajectory that brings it near, but not precisely above, the aluminum can. Then the EF servoing brings the end effector directly above the can. In the supporting video, the can is then moved and the end effector tracks it dynamically.

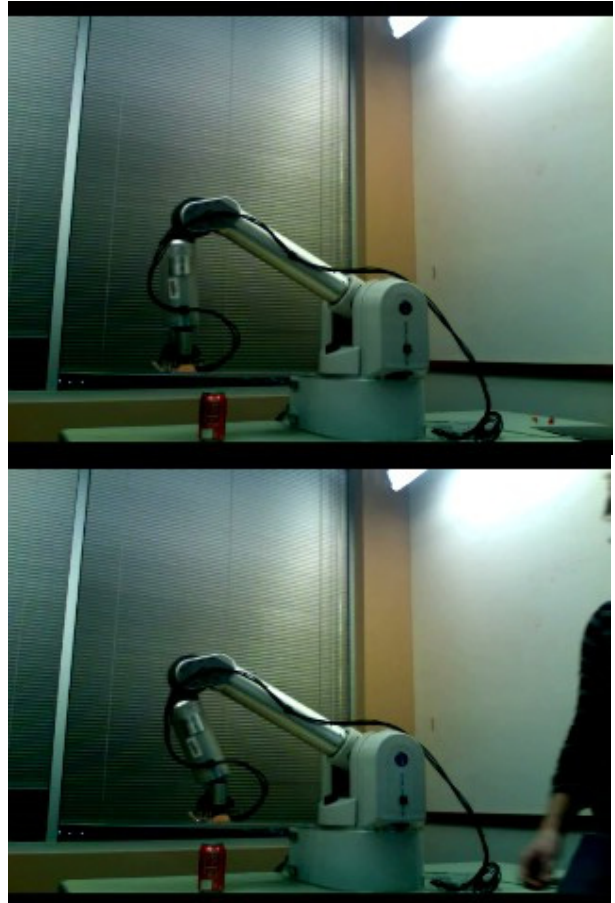


Fig. 6: EF servoing of arm end effector. The arm executes a pre-planned trajectory which brings it near the object. However, the end effector is not well-aligned with the object (upper image), which in practice might occur because of sensing or actuation errors. Using EF servoing, the arm corrects the misalignment (lower image).

Figures 7, 8, and 9 show the “basins of attraction” for an aluminum can, apple (about 10cm diameter), and small tomato (about 4cm diameter). In the plots, the object is located at (0,0) in the (x,y) plane. The z value indicated is the height of the sensor electrodes above the top of the object. The end effector was started at each location on a 5 cm spaced grid that is 30 cm x 30 cm in extent. If the end effector successfully servos to the target object at (0,0), a circle is plotted in the figure. Thus the region with circles plotted represents the basin of attraction, within which the end effector will be able to detect and servo to the object. If the arm is not able to servo to the object from any point in one of the z planes, that plane was not plotted. The figures

indicate that the aluminum can provides the best signal, followed by the apple, and then the small tomato. The aluminum can is detected reliably through most of the 40 cm x 40 cm region if the end effector height above the object is 14 cm or lower.

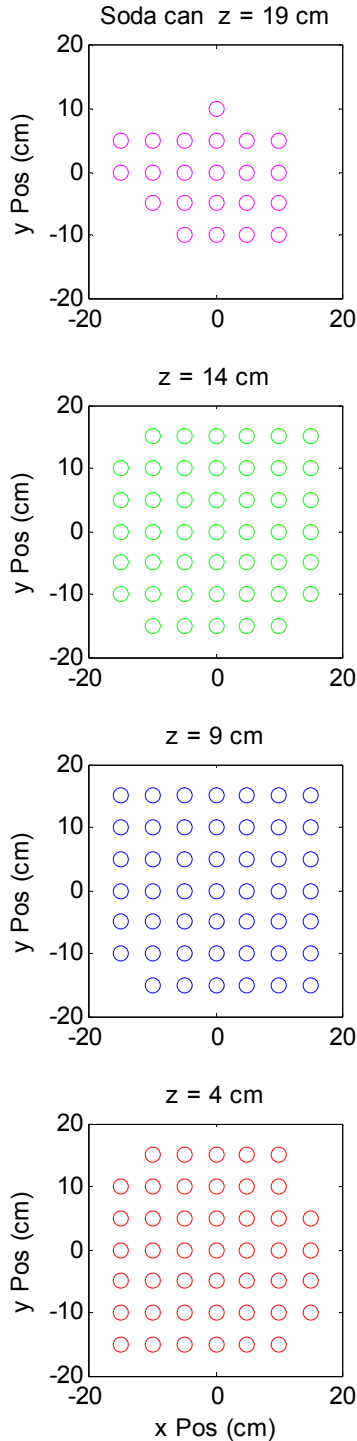


Fig. 7: Basin of attraction for aluminum can. Note that the horizontal axis label “x Pos (cm)” appears just for the bottom figure.

When the height is 19cm, the horizontal field of view begins to diminish. The horizontal field of view for the apple is somewhat smaller even at $z = 4$ cm. At $z = 9$ cm, successful servoing can occur, but in a smaller region (5 cm to 10 cm in extent). The small tomato was only successfully served at $z = 4$ cm. In this case the horizontal field of view was about 10 cm.

For the manipulation tasks we intend to use this technique for, these detection regions are sufficiently large. We envision using this method to generate small position corrections, so even the smallest 4 cm detection range should be sufficient in many cases.

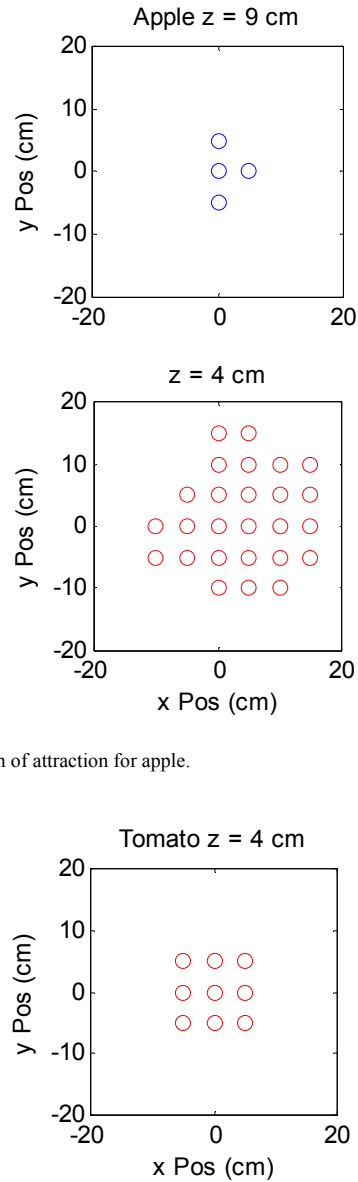


Fig. 8: Basin of attraction for apple.

Fig. 9: Basin of attraction for small tomato (4cm x 4cm x 4 cm).

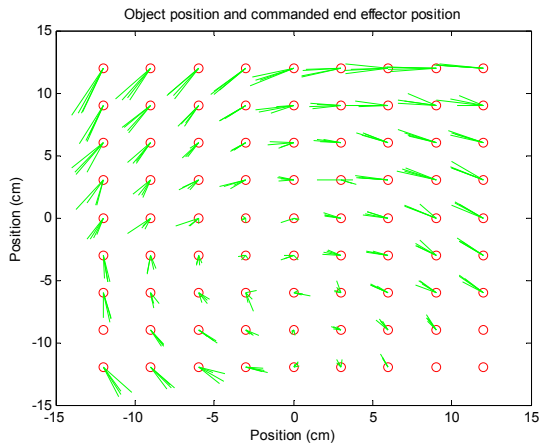


Fig. 10: True object position (red circles) and position command sent to Virtual Series Elastic Actuator controller (ends of green segments not contacting the red circles) required to achieve EF equilibrium. The can was placed at each of the 81 locations on a 3cm-spaced grid, shown as circles in the figure. Starting from (0,0) the arm servoed to each can position 4 times. The line segments show the position commands sent to the VSEA controller that resulted in an the EF error signal near zero. The spread of the “bundles” of 4 segments is at most 2 cm, which indicates the precision of this procedure (about 2cm). See the text for an explanation of the larger apparent systematic errors (i.e. the length of the green segments).

Fig. 10 shows true object position (red circles) and position command sent to Virtual Series Elastic Actuator controller (ends of green segments not contacting the red circles) required to achieve EF equilibrium. The can was placed at each of the 81 locations on a 3cm-spaced grid, shown as circles in the figure. Starting from (0,0) the arm servoed to each can position 4 times. The line segments show the position commands sent to the VSEA controller that resulted in an EF error signal near zero. The spread of the “bundles” of 4 segments is at most 2 cm, which indicates the precision of this procedure (about 2cm). The larger apparent systematic errors (i.e. the fact that some of the green segments are 3cm to 5cm in length) is due mostly, we believe, to the VSEA controller. Since the VSEA controller implements compliant dynamics, gravity can cause the actual arm configuration to droop slightly away from the position commanded to the VSEA controller. Thus, the plot above suggests that our method is accurate only to within 5cm or so.

However, we believe that in actuality the method is more accurate than suggested by the length of some of the segments in Fig. 10. To show this clearly, one would collect the actual arm configuration recorded by the arm’s encoders, and then solve the forward kinematics for the end effector position. One could then produce a plot that showed actual object position and actual EF servoed position (rather than what is actually plotted: the command that was sent to the VSEA controller that caused it to zero the EF sensor imbalance). For the most reliable assessment of this method’s precision and accuracy, one might use a laser

rangefinder and/or vision system to measure both the true object position, and end effector EF-equilibrium position.

One natural question about this work is whether it is applicable to asymmetric objects. For the arm servoing experiment presented in this section, the arm would simply servo to a “centroid” location defined by the field measurements, but would track the motion of the object in the same manner.

VI. CONCLUSION AND FUTURE WORK

This paper presented two experiments in which electric field measurements provided error signals for closed loop control in manipulation tasks. In the first, a robot hand pre-shapes to objects by servoing each finger independently. In the second, an arm servoed the position of its end effector to align with an object.

In future work, we intend to combine these two experiments by mounting the EF sensing hand on the arm. The arm could first be moved such that the hand is approximately aligned with the target object. Then the fingers could be pre-shaped to the object. Finally the fingers could be closed to grasp the object. This set up could also handle asymmetric objects more effectively.

If Electric Field Pretouch does prove useful for manipulation, it will be worth exploring additional pretouch mechanisms that can detect materials that EF sensing cannot. Implementing multiple pretouch mechanisms in parallel would allow a larger class of objects to be used, and would even provide some material composition information.

ACKNOWLEDGMENTS

Thanks to Mike Vande Weghe for the Barrett Hand fingertip geometry. We thank Siddhartha Srinivasa for helpful conversations.

REFERENCES

- [1] S. A. Hutchinson, G. D. Hager, and P. I. Corke. A tutorial on visual servo control. *IEEE Trans. Robot. Automat.*, 12(5):651–670, Oct. 1996.
- [2] Smith, J.R., E. Garcia, R. Wistort, G. Krishnamoorthy. "Electric field imaging pretouch for robotic graspers," *Proceedings of IEEE/RSJ International Conference on Intelligent Robots and Systems, IROS 2007*, pp.676-683, Oct. 29 2007-Nov. 2 2007.
- [3] Smith, J.R., "Electric Field Imaging," Ph.D. Dissertation, Massachusetts Institute of Technology
- [4] Novak J., L., Feddema, I., T., "A capacitance-based proximity sensor for whole arm obstacle avoidance," *Proceedings of the 1992 IEEE International Conference on Robotics and Automation*, pp 1307-1314, Nice, France, 1992.
- [5] N. Karlsson, "Theory and Application of a Capacitive Sensor for Safeguarding in Industry," *Proceedings of IEEE Instr. and Msmt. Technology Conf.--IMTC 94, Hammamatsu, Japan, May, 1994*
- [6] D.J. Schmitt, J.L. Novak, G.P. Starr and J.E. Maslowski, *Real-Time Seam Tracking for Rocket Thrust Chamber Manufacturing*, 1994 *IEEE Robotics and Automation Proceedings*.
- [7] G.F. Mauer, "An End-Effector Based Imaging Proximity Sensor," *Journal of Robotic Systems*, 1989, pp301-316, Wiley & Sons.
- [8] J.R. Solberg, K.M. Lynch, M.A. MacIver, "Robotic Electrolocation: Active Underwater Target Localization with Electric Fields," *Proceedings of the 2007 International Conference on Robotics and Automation (ICRA) April 10-14, 2007, Rome Italy*.